

# Dalton Transactions

An international journal of inorganic chemistry  
rsc.li/dalton



Themed issue: Frontiers in Radionuclide Imaging and Therapy

ISSN 1477-9226



PAPER

Gilles Gasser, Adoración G. Quiroga, António Paulo *et al.*  
Combining imaging and anticancer properties with new heterobimetallic  
Pt(II)/M(I) (M = Re,  $^{99m}\text{Tc}$ ) complexes



Cite this: *Dalton Trans.*, 2017, **46**, 14523

## Combining imaging and anticancer properties with new heterobimetallic Pt(II)/M(I) (M = Re, <sup>99m</sup>Tc) complexes†

Leticia Quental,<sup>a</sup> Paula Raposinho,<sup>a</sup> Filipa Mendes,<sup>a</sup> Isabel Santos,<sup>a</sup> Carmen Navarro-Ranninger,<sup>b</sup> Amparo Alvarez-Valdes,<sup>b</sup> Huaiyi Huang,<sup>c,d</sup> Hui Chao,<sup>d</sup> Riccardo Rubbiani,<sup>c</sup> Gilles Gasser,<sup>\*e</sup> Adoración G. Quiroga<sup>\*b</sup> and António Paulo<sup>\*a</sup>

In this article, we report on the development of new metal-based anticancer agents with imaging, chemotherapeutic and photosensitizing properties. Hence, a new heterobimetallic complex (**Pt-LQ-Re**) was prepared by connecting a non-conventional *trans*-chlorido Pt(II) complex to a photoactive Re tricarbonyl unit (**LQ-Re**), which can be replaced by <sup>99m</sup>Tc to allow for *in vivo* imaging. We describe the photophysical and biological properties of the new complexes, in the dark and upon light irradiation (DNA interaction, cellular localization and uptake, and cytotoxicity). Furthermore, planar scintigraphic images of mice injected with **Pt-LQ-Tc** clearly showed that the radioactive compound is taken up by the excretory system organs, namely liver and kidneys, without significant retention in other tissues. All in all, the strategy of conjugating a chemotherapeutic compound with a PDT photosensitizer endows the resulting complexes with an intrinsic cytotoxic activity in the dark, driven by the non-classical platinum core, and a selective activity upon light irradiation. Most importantly, the possibility of integrating a SPECT imaging radiometal (<sup>99m</sup>Tc) in the structure of these new heterobimetallic complexes might allow for *in vivo* non-invasive visualization of their tumoral accumulation, a crucial issue to predict therapeutic outcomes.

Received 5th January 2017,  
Accepted 25th January 2017

DOI: 10.1039/c7dt00043j

rsc.li/dalton

## Introduction

Anticancer therapeutic approaches relying on a single therapeutic modality (e.g. chemotherapy, external radiotherapy, etc.) and/or involving the administration of a single drug (e.g. chemotherapeutic, radiosensitizer, etc.) very often do not lead to a satisfactory curative outcome, mostly due to acquired chemo- and radio-resistance or the occurrence of undesired side effects. Different strategies have been applied over the past few years to overcome these drawbacks, including the design of more selective and target-specific anticancer drugs or the com-

bination of different independent therapeutic modalities. An example of such a combination may involve chemotherapy and photodynamic therapy (PDT).<sup>1,2</sup> PDT is a clinically approved technique, which involves light-induced generation of cytotoxic singlet oxygen (<sup>1</sup>O<sub>2</sub>) from endogenous <sup>3</sup>O<sub>2</sub> and/or other reactive oxygen species (ROS), mediated by a photosensitizer. PDT is, for example, used for the treatment of certain malignant tissues. Compared with other conventional anticancer treatments, PDT has many advantages, namely spatial and temporal control and the possibility of repeated doses.<sup>1,2</sup>

At a first glance, the more obvious and straightforward strategy for a dual chemo/PDT therapeutic approach is based on the administration of two individually different chemotherapeutic and photosensitizing agents already in clinical use. However, the two individual agents will necessarily show different pharmacokinetics and different tumor targeting ability. To circumvent these drawbacks, the merging of the cytotoxic and photosensitizing units into the same chemical entity is an attractive alternative that has been investigated using mainly porphyrin derivatives as the photosensitizer unit.<sup>1,2</sup> Importantly, the exploration of novel metal-based “hybrid” anticancer agents, acting at the same time as a cytotoxic drug and as a PDT photosensitizer, might open new avenues in the design of these types of agents, profiting from

<sup>a</sup>Centro de Ciências e Tecnologias Nucleares, Instituto Superior Técnico, Universidade de Lisboa, Estrada Nacional 10, 2695-066 Bobadela LRS, Portugal. E-mail: apaulo@ctn.tecnico.ulisboa.pt

<sup>b</sup>Departamento de Química Inorgánica and IAdChem., Universidad Autónoma de Madrid, ES-28049 Madrid, Spain. E-mail: adoracion.gomez@uam.es

<sup>c</sup>Department of Chemistry, University of Zurich, CH-8057 Zurich, Switzerland

<sup>d</sup>School of Chemistry and Chemical Engineering, Sun Yat-Sen University, Guangzhou, 510275, China. E-mail: ceschh@mail.sysu.edu.cn

<sup>e</sup>Chimie ParisTech, PSL Research University, Laboratory for Inorganic Chemical Biology, F-75005 Paris, France. E-mail: gilles.gasser@chimie-paristech.fr

†Electronic supplementary information (ESI) available: Biodistribution data, characterization spectra, HPLC chromatograms and pulse field gel electrophoresis. See DOI: 10.1039/c7dt00043j

the variety of structural motifs and the diversity of the physico-chemical properties and biological characteristics exhibited by metal complexes.

In the last few years, research interests of several groups have been focused on two types of compounds that can be used as tools to achieve “hybrid” metal-based drugs: (a) organometallic Re(I)/Tc(I) compounds to obtain photosensitizers for PDT and radiopharmaceuticals for nuclear imaging or radionuclide therapy<sup>1,3–6</sup> and (b) platinum compounds to obtain powerful anticancer agents.<sup>7</sup> These two classes of compounds can also allow for the development of novel agents combining diagnostic and therapeutic tools (theranostic agents), which has emerged as a new approach to fight cancer over the last decade and, in consequence, became a major goal in medicinal/medical research.<sup>1</sup>

The interest in the use of Re(I) tricarbonyl complexes as photosensitizers for PDT purposes is relatively recent.<sup>3,6,8,9</sup> Re(I) complexes have been mainly explored as luminescent probes because of their photophysical properties, like long lifetimes, polarized emission and large Stokes shifts.<sup>10–15</sup> In particular, those having the core *fac*-[Re(CO)<sub>3</sub>]<sup>+</sup> with ligands derived from *N,N'*-bis[(quinolin-2-yl)methyl]amine are endowed with luminescence properties that might allow for visualization of their intracellular trafficking by fluorescence microscopy.<sup>3,8</sup> On the other hand, the <sup>99m</sup>Tc analogues of Re(CO)<sub>3</sub> complexes can be easily prepared (based on their chemical similarities) to perform *in vivo* radioimaging, bridging the gap between cellular, animal and human imaging studies.<sup>8,13–17</sup> <sup>99m</sup>Tc is employed to obtain a variety of radiopharmaceuticals that are in clinical use for early detection of several diseases by means of Single Photon Emission Computed Tomography (SPECT).<sup>18,19</sup> The longstanding and unsurpassed success of <sup>99m</sup>Tc in medical imaging is due to its commercial availability and its optimal features for imaging, among other factors. These include a short half-life of 6.02 h that is long enough to allow for the preparation of the radiopharmaceuticals by <sup>99m</sup>Tc-labelling of commercially available freeze-dried kits<sup>20</sup> and the *in vivo* accumulation in the target tissue/organ, but it is sufficiently short to avoid a long term exposition of the patient to the radiation dose.

In summary, organometallic M(I) (M = <sup>99m</sup>Tc or Re) complexes have useful and unique features for biomedical applications: (i) chemical robustness of the *fac*-[M(CO)<sub>3</sub>]<sup>+</sup> core; (ii) well-studied coordination chemistry with a variety of chelating ligands including targeting molecules;<sup>17,21–23</sup> (iii) possible application in the design of metal-based cancer theranostic agents where Re complexes can be incorporated into a cytotoxic or photosensitizing entity that will exert a therapeutic effect, while the <sup>99m</sup>Tc congeners are part of the corresponding imaging tool for *in vivo* assessment of tumor accumulation.<sup>24–26</sup> Due to its radioactive properties, <sup>99m</sup>Tc can only be obtained in small amounts (<1 μM) that are well below the minimum threshold concentrations that are required for a biological response. In brief, isostructural Re and <sup>99m</sup>Tc complexes allow for a theranostic approach of cancer, where the Re complexes exert the therapeutic effects

and the <sup>99m</sup>Tc congeners are used solely for imaging/diagnostic purposes.

Platinum compounds, namely cisplatin, carboplatin and oxaliplatin, are used in the clinic as powerful anticancer drugs. However, they are responsible for severe side effects and there is undoubtedly a growing need for novel compounds of the same or higher efficiency with reduced side effects. Non-conventional drug design grew as an interesting alternative to fulfill this need, and *trans*-chlorido Pt(II) complexes appeared as one of these non-classical examples. Interestingly, from the analysis of their structures, they were not expected to be active against cancer cells. However, they were shown to be highly cytotoxic.<sup>27</sup>

In this study, we decided to follow the idea of multifunctional metal-based compounds that combine therapeutics and diagnosis in the same chemical entity, to obtain new anticancer drugs suitable for a theranostic approach. For this purpose, we developed new heterobimetallic complexes with a *trans*-chlorido Pt(II) moiety and a Re(I)/<sup>99m</sup>Tc(I) tricarbonyl core. The rationale behind this concept is the central role of Pt(II) complexes in the development of chemotherapeutic drugs, the importance of <sup>99m</sup>Tc for *in vivo* tumor imaging and the possibility of using the Re(CO)<sub>3</sub> core in PDT.

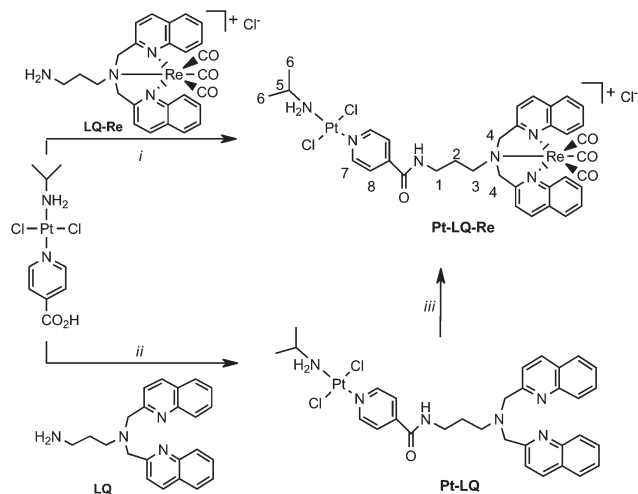
Based on our results that showed that some non-classical *trans*-Pt(II) complexes with isopropylamine and pyridine derivatives are active in cisplatin-resistant cell lines,<sup>27,28</sup> we selected these types of compounds to synthesize the new Pt(II)/M(I) (M = Re, <sup>99m</sup>Tc) heterobimetallic complexes. For the corresponding organometallic moiety, we have focused on *N,N'*-bis[(quinolin-2-yl)methyl]amine M(CO)<sub>3</sub> derivatives containing an *n*-propylamine pendant arm because this class of compounds can present remarkable phototoxic properties and, importantly, since the cold Re atom can be efficiently replaced with <sup>99m</sup>Tc, as mentioned above.<sup>3,8,13–17</sup> We expected to obtain complexes with cytotoxic activity, PDT photosensitizing properties and, more importantly, allowing *in vivo* imaging. To assemble this new family of complexes, our strategy involved 4-picolinic acid as a bridging element between the Pt(II) metallic core and the bis(quinoline)amine moiety, which can react with the Re(I)/<sup>99m</sup>Tc(I) tricarbonyl core to afford the aforementioned organometallic compounds. Herein, we report the synthesis and characterization of the resulting heterobimetallic Pt(II)/M(I) (M = Re, <sup>99m</sup>Tc) complexes, as well as the study of their photophysical properties and their *in vitro* and *in vivo* biological evaluation (cytotoxicity, photocytotoxicity, cell uptake assays, and biodistribution in normal mice).

## Results and discussion

### Chemical synthesis: ligands and non-radioactive complexes (Re and Pt)

As indicated in Scheme 1, two different approaches were investigated to obtain the final heterobimetallic compound **Pt-LQ-Re**:





**Scheme 1** Synthesis of Pt-LQ-Re. Approach 1: (i) DIPEA, NHS, EDC, DMF, 16 h, r.t. ( $\eta$  = 19%). Approach 2: (ii) DIPEA, NHS, EDC, DCM, 16 h ( $\eta$  = 58%); (iii) Re(CO)<sub>5</sub>Cl, THF, o.n., r.t. ( $\eta$  = 29%).

**Approach 1.** Amidation reaction between *trans*-[PtCl<sub>2</sub>(isopropylamine)(4-picolinic acid)] (*trans*-[PtCl<sub>2</sub>ipa(pic)]) and *fac*-tricarbonyl[*N,N'*-bis(quinolin-2-ylmethyl)propane-1,3-diamine]rhenium(i) (LQ-Re) and

**Approach 2.** Initial coupling of the bifunctional chelator *N,N'*-bis(quinolin-2-ylmethyl)propane-1,3-diamine (LQ) to *trans*-[PtCl<sub>2</sub>ipa(pic)], followed by complexation of the *fac*-[Re(CO)<sub>3</sub>]<sup>+</sup> core by the resulting conjugate Pt-LQ.

**Approach 1.** This approach was envisaged to avoid the involvement of the free bis(quinoline) chelator (LQ) in competitive coordination reactions with the Pt(II) core, allowing therefore for a more controlled process to obtain the desired Pt-Re heterobimetallic complex. This approach starts with the synthesis of LQ-Re that should be subsequently applied in the amide coupling with *trans*-[PtCl<sub>2</sub>ipa(pic)]. Initially, the synthesis of LQ-Re was attempted by reacting a methanol solution of LQ with a stoichiometric amount of [Re(CO)<sub>3</sub>(H<sub>2</sub>O)<sub>3</sub>]Br. This synthetic method was considered due to the highest reactivity of [Re(CO)<sub>3</sub>(H<sub>2</sub>O)<sub>3</sub>]Br compared with more “classical” pentacarbonyl precursors, like [Re(CO)<sub>5</sub>X] (X = Cl, Br).<sup>29</sup> This enhanced reactivity reflects the high lability of the coordinated water molecules and allows for the use of milder conditions to synthesize Re(i) tricarbonyl complexes with tridentate chelators. The reaction of LQ with [Re(CO)<sub>3</sub>(H<sub>2</sub>O)<sub>3</sub>]Br led to the desired complex, which was obtained in high yield (83%) with bromide as the counter-ion ([LQ-Re]Br). The coupling of [LQ-Re]Br to *trans*-[PtCl<sub>2</sub>ipa(pic)] proceeded well upon activation of the free carboxylic acid of the later with *N*-hydroxysuccinimide (NHS). However, the amide coupling reaction was followed by metathesis reactions involving the Pt(II) core that led to the replacement of the coordinated chloride by bromide with the formation of a mixture of heterobimetallic complexes: the desired Pt-LQ-Re and the congeners presenting the *trans*-[PtClBr(ipa)(pic)] and *trans*-[PtBr<sub>2</sub>(ipa)(pic)] units. The formation of these three heterobimetallic complexes was

corroborated by ESI-MS analysis of one aliquot of the reaction mixture and by the presence of three signals in its <sup>195</sup>Pt NMR spectrum (Fig. S1†).

These results prompted us to synthesize LQ-Re by reacting [Re(CO)<sub>5</sub>Cl] with LQ in refluxing THF. This synthetic method gave [LQ-Re]Cl in high yield (69%), after HPLC purification to remove any unreacted starting materials. As shown in Scheme 1, the coupling reaction of [LQ-Re]Cl with *trans*-[PtCl<sub>2</sub>ipa(pic)] afforded the desired Pt-LQ-Re compound, which was obtained as a light orange oil, after HPLC purification, with a relatively low yield of 19%. In this case, the <sup>195</sup>Pt NMR and ESI-MS spectra of the isolated Pt-LQ-Re were consistent with the presence of a single Pt(II) species displaying a PtCl<sub>2</sub> environment, as discussed in more detail below.

**Approach 2.** In the second approach, it was taken into consideration that the radioactive congener of Pt-LQ-Re, *i.e.* Pt-LQ-Tc, should be obtained in a similar manner, *i.e.* by reacting Pt-LQ with *fac*-[<sup>99m</sup>Tc(CO)<sub>3</sub>(H<sub>2</sub>O)<sub>3</sub>]<sup>+</sup> (see below). Due to the similar chemical behavior of Re(i) and Tc(i) tricarbonyl complexes, the study of the reaction of Pt-LQ with [Re(CO)<sub>3</sub>(H<sub>2</sub>O)<sub>3</sub>]Br to obtain Pt-LQ-Re will give important hints about the possibility of synthesizing the radioactive congener Pt-LQ-Tc at the low concentrations of <sup>99m</sup>Tc (<10<sup>-6</sup> M, no carrier added level) that are characteristic of <sup>99m</sup>Tc-radiopharmaceuticals.

To obtain the Pt-LQ intermediate, LQ was reacted with the NHS-activated *trans*-[PtCl<sub>2</sub>ipa(pic)] (Scheme 1). Pt-LQ was recovered as an orange oil in moderate yield (58%) after semi-preparative HPLC purification. Thereafter, the ability of Pt-LQ to coordinate the *fac*-[Re(CO)<sub>3</sub>]<sup>+</sup> core was investigated. For this purpose, the reaction of Pt-LQ with [Re(CO)<sub>3</sub>(H<sub>2</sub>O)<sub>3</sub>]Br was first studied. [Re(CO)<sub>3</sub>(H<sub>2</sub>O)<sub>3</sub>]<sup>+</sup> readily reacts with Pt-LQ, as indicated by HPLC analysis of the reaction mixture. However the complexation of *fac*-[Re(CO)<sub>3</sub>]<sup>+</sup> by Pt-LQ is followed by the replacement of the coordinated chlorides by bromide with the formation of a mixture of heterobimetallic Pt(II) halides containing the *trans*-[Pt(X)(Y)ipa(pic)] (X = Y = Cl; X = Cl, Y = Br; X = Y = Br) units, as indicated by ESI-MS analysis. Purification of the different Pt(II) complexes in this mixture by HPLC was attempted, but without success. Finally, as shown in Scheme 1, Pt-LQ was reacted with [Re(CO)<sub>5</sub>Cl] in refluxing THF. This synthetic method allowed for the synthesis of the chloride salt of Pt-LQ-Re in moderate yield (29%).

Pt-LQ-Re and all the new compounds involved in this study were analyzed by different spectroscopic techniques (IR and <sup>1</sup>H, <sup>13</sup>C and <sup>195</sup>Pt-NMR) and mass spectrometry, allowing for the unambiguous identification of their chemical structures (see the Experimental section for detailed procedures and characterization). Concisely, the <sup>1</sup>H-NMR and IR data collected for LQ-Re confirmed the proposed formulation and are consistent with those reported recently for similar bis(quinoline) Re(i) tricarbonyl complexes.<sup>2,30</sup> In particular, the methylenic H-4 protons (see Scheme 1 for atom numbering) give rise to a doublet in the <sup>1</sup>H-NMR spectrum of LQ-Re, consistent with an AB spin pattern and with the coordination to the Re(i) centre that renders these protons diastereotopic. The IR spectrum of LQ-Re shows intense absorption bands in the range 1897–2018 cm<sup>-1</sup>

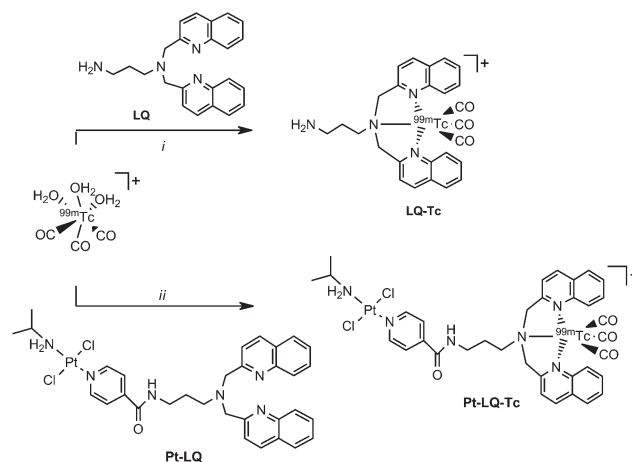
that are easily assigned to the  $\nu(\text{C}\equiv\text{O})$  stretching modes by comparison with the values previously reported for such bands in other related Re(I) tricarbonyl complexes.<sup>30,31</sup>

The  $^1\text{H}$ -NMR spectrum of **Pt-LQ** confirms the linkage of **LQ** to the picolinic acid of the original *trans* complex without the release of the ligands coordinated to Pt(II). The spectrum shows the presence of the signals of the aliphatic protons of isopropylamine at 3.39 and 1.39 ppm. The spectrum also shows the presence of aromatic signals arising from the protons of the functionalized picolinic acid (appearing at 7.37 and 8.75 ppm) and the bis(quinoline) moiety (twelve aromatic protons at 7.60–8.22 ppm), as well as aliphatic signals due to the methylenic protons of the *n*-propylamine pendant arm.

The IR spectrum of **Pt-LQ-Re** shows intense  $\nu(\text{C}\equiv\text{O})$  bands between 1975 and 2025  $\text{cm}^{-1}$ , which confirms the presence of the *fac*-[Re(CO)<sub>3</sub>]<sup>+</sup> core in this heterobimetallic complex. Consistently, the  $^1\text{H}$ -NMR spectrum of **Pt-LQ-Re** corresponds almost to the sum of the spectra of **Pt-LQ** and **LQ-Re**, reflecting the assembly of the two metal cores (Fig. S2 and S3†). The most striking difference is in the chemical shifts of the aromatic protons of picolinic acid, which are significantly high-field shifted in the case of **Pt-LQ** if compared with **Pt-LQ-Re** (7.37 and 8.75 ppm vs. 7.92 and 8.98 ppm, respectively). This shift towards the high-field is possibly caused by the ring current shielding effects of the intramolecular  $\pi$ - $\pi$  stacking interactions between the picolinic acid aromatic ring and the dangling quinolone aromatic rings. The metalation of bis(quinoline) hinders such intramolecular  $\pi$ - $\pi$  stacking and, for this reason, the chemical shifts of the picolinic acid in **Pt-LQ-Re** are almost coincident with those of the parental complex *trans*-[PtCl<sub>2</sub>ipa(pic)].<sup>27</sup> Finally, the  $^{195}\text{Pt}$ -NMR spectra of solutions of **Pt-LQ** and **Pt-LQ-Re** exhibited only one signal at similar chemical shifts consistent with the proposed coordination spheres (−2098.39 and −2098.20 ppm, respectively).<sup>27,32</sup>  $^1\text{H}$  and  $^{13}\text{C}$ -NMR spectra assignment were double checked by two-dimensional experiments using homo- and heteronuclear techniques, such as DEPT-135,  $^1\text{H}$ - $^1\text{H}$  COSY and  $^1\text{H}$ - $^{13}\text{C}$  HSQC. The ESI-MS spectra of **LQ-Re**, **Pt-LQ** and **Pt-LQ-Re** showed peaks and isotopic patterns consistent with the expected molecular ions.

#### Synthesis, characterization and *in vitro* evaluation of $^{99\text{m}}\text{Tc}$ complexes

The synthesis of the  $^{99\text{m}}\text{Tc}$  complexes, namely **LQ-Tc** and **Pt-LQ-Tc**, was performed in aqueous saline solution at pH  $\approx$  5 by reaction of *fac*-[ $^{99\text{m}}\text{Tc}(\text{CO})_3(\text{H}_2\text{O})_3$ ]<sup>+</sup> with **LQ** ( $5 \times 10^{-4}$  M final concentration) and **Pt-LQ** ( $10^{-3}$  M final concentration) for 60 min, at 50 °C and 60 °C, respectively (Scheme 2). To our knowledge, **Pt-LQ-Tc** is the first reported example of a  $^{99\text{m}}\text{Tc}$ /Pt heterobimetallic complex. Its synthesis was achieved in reasonably high radiochemical yield (>90%) after appropriate optimization of the reaction conditions, such as the ligand concentration, pH and temperature. Noticeably, the presence of the Pt(II) complex had a positive influence on the radiolabeling reaction, as **Pt-LQ-Tc** was typically obtained in a higher radiochemical yield than **LQ-Tc** (90% vs. 50% yield). However, the synthesis of **Pt-LQ-Tc** is strongly pH-dependent. When the



**Scheme 2** Synthesis of the  $^{99\text{m}}\text{Tc}$  complexes. (i) 0.9% NaCl, 50 °C, 1 h, pH = 5 ( $\eta$  = 50%); (ii) 0.9% NaCl, 60 °C, 1 h, pH = 5 ( $\eta$  > 90%).

reactions were carried out at neutral pH the formation of two major radioactive species was observed in addition to the desired complex that was formed, under these conditions, only with *ca.* 30% yield. By performing the reaction at pH 5, the formation of these two radiochemical impurities, resulting most probably from hydrolysis processes involving the *trans*-PtCl<sub>2</sub> core, was almost eliminated.

The chemical identity of **LQ-Tc** and **Pt-LQ-Tc** was ascertained by comparison of their HPLC profiles with the corresponding Re surrogates, as exemplified for **Pt-LQ-Tc** in Fig. S4A.† For this purpose, the HPLC-purified samples of these  $^{99\text{m}}\text{Tc}$ -containing compounds were used. The *in vitro* and *in vivo* studies reported below for **LQ-Tc** and **Pt-LQ-Tc** were also always performed using the HPLC-purified samples of these compounds.

The *in vitro* evaluation of **LQ-Tc** and **Pt-LQ-Tc** comprised the measurement of their lipophilicity and the study of their stability in different media (PBS, human serum, and cell culture medium) with relevance to the biological studies that were performed for these compounds and for the Re congeners (**LQ-Re** of **Pt-LQ-Re**).

The study of the stability of the complexes **LQ-Tc** and **Pt-LQ-Tc** in the presence of the different challenging media was performed by co-incubating each tested compound with the desired medium at 37 °C for different intervals of time, followed by radio-HPLC analysis of the reaction mixtures. Both compounds exhibited a high stability under all evaluated challenging conditions, without the formation of new radiochemical species until 6 h of incubation, as exemplified for **Pt-LQ-Tc**, in the presence of human serum (Fig. S4B†). Overall, the *in vitro* evaluation of **Pt-LQ-Tc** has shown that it is a quite robust complex, under several biological conditions. It is reasonable to assume that the same is valid for the congener **Pt-LQ-Re**, that displays the same Pt(II) core and a *fac*-[Re(CO)<sub>3</sub>]<sup>+</sup> core chemically related to *fac*-[Tc(CO)<sub>3</sub>]<sup>+</sup>.

The lipophilicity of **LQ-Tc** and **Pt-LQ-Tc** was assessed by measurement of the respective log  $P_o/P_w$  values (*n*-octanol/

0.1 M PBS, pH = 7.4) using the multiple back-extraction method. The obtained  $\log P_o/P_w$  values of  $0.57 \pm 0.02$  and  $1.44 \pm 0.04$ , respectively, show that both compounds have a lipophilic character. Other cationic lipophilic complexes described in the literature with favorable cell uptake have  $\log P_o/P_w$  in the same range of values, e.g. the promising myocardial agent  $^{99m}\text{Tc}$ -TMEOP ( $0.61 \pm 0.04$ ).<sup>33</sup> **Pt-LQ-Tc** is more lipophilic than **LQ-Tc**, due to the introduction of a neutral Pt(II) core that contains coordinated organic ligands. By contrast, the heterobimetallic **Pt-LQ-Tc** is much more lipophilic than Pt drugs in clinical use, like cisplatin, carboplatin or oxaliplatin, which display  $\log P_o/P_w$  values ranging between  $-2.5$  and  $-1.5$ .<sup>34,35</sup>

### Photophysical properties

*N,N'*-Bis[(quinolin-2-yl)methyl]amine Re(I) complexes possess favorable properties as luminescent probes.<sup>3,8</sup> Therefore, to assess whether the new heterobimetallic complexes would present similar characteristics, the luminescence properties of the different complexes were studied and are summarized in Table 1; the respective electronic and emission spectra are presented in Fig. S5 and S6.†

All complexes showed a weak absorption in the visible region (400–800 nm). The absorbance between 200 and 250 nm was almost the same for the three compounds, suggesting that it is induced by the ligand. **LQ-Re** exhibited a UV absorbance between 280 and 350 nm with a maximum at 322 nm (Fig. S5†). These features are comparable with structurally similar Re(I) complexes<sup>36</sup> and are the result of a metal-to-ligand charge-transfer (MLCT:  $d_\pi(\text{Re}) \rightarrow \pi^*(\text{ligand})$ ).<sup>37</sup> As expected, the absorbance spectrum of **Pt-LQ-Re** was found to be a mixture of the absorbance spectra of **LQ-Re** and **Pt-LQ**.

Upon excitation at 350 nm, **LQ-Re** showed two distinct emission bands, typical of Re(I) complexes (Fig. S6†).<sup>38</sup> The high-energy transition (430 nm) was assigned to ligand-centered fluorescence, whilst the lower energy transition (560 nm) originated from a <sup>3</sup>MLCT phosphorescence state. **Pt-LQ** presented only one emission peak at 430 nm, which comes from the **LQ** ligand. The heterobimetallic **Pt-LQ-Re** complex showed a broad emission band between 400 and 650 nm. Luminescence lifetimes were also evaluated (Table 1) and for **LQ-Re** the value obtained was similar to the values of other rhenium tricarbonyl bisquinoline complexes.<sup>37</sup> The lifetime of **Pt-LQ** was almost identical to the one of **LQ-Re** (around 700 ns), however when the two metals are present the lifetime falls down to 509 ns.

The luminescence quantum yields ( $\Phi_{\text{em}}$ ) were evaluated to understand the behavior of the compounds in the excited state. The  $\Phi_{\text{em}}$  for all complexes was evaluated in DMSO (Table 1) and compared with  $[\text{Ru}(\text{bipy})_3]^{2+}$  in water ( $\Phi_{\text{em}} = 4.0\%$ ).<sup>39</sup> The quantum yields of all complexes were smaller than 1% (Table 1). In the case of **Pt-LQ-Re** and **LQ-Re**, these results are in agreement with the data obtained for other Re(I) tricarbonyl complexes described in the literature.<sup>3,12</sup>

### Singlet oxygen sensitization

A quantitative evaluation of the singlet oxygen  $^1\text{O}_2$  ( $^1\Delta_g$ ) production upon irradiation at 350 nm was performed to assess the potential of these complexes as photosensitizers in PDT. An indirect method was used in both PBS (with 10 mM histidine) and acetonitrile (with 12 mM imidazole) solutions.  $^1\text{O}_2$  can react with an imidazole derivative to form a *trans*-annular peroxide adduct, which is able to quench the absorbance of *p*-nitrosodimethyl aniline (RNO).<sup>3,40,41</sup> The  $^1\text{O}_2$  production quantum yields were evaluated by comparison with a reference molecule phenalenone ( $\Phi(^1\Delta_g) = 95\%$ ).<sup>41</sup> The results obtained are shown in Table 1. **LQ-Re** exhibited the highest singlet oxygen generation efficiency among the three compounds, both in PBS and acetonitrile. The quantum yields in acetonitrile were higher than those obtained in PBS solution. These results were comparable with previously reported data on a very similar complex.<sup>3</sup> Interestingly, the introduction of a platinum(II) complex to the structure of **LQ-Re** decreased the singlet oxygen generation efficiency of **LQ-Re**, particularly in the case of the values obtained in acetonitrile. These values are even lower than the ones observed for **Pt-LQ**.

### Dark- and photo-toxicity

The dark- and photo-toxicity of the complexes **LQ-Re**, **Pt-LQ** and **Pt-LQ-Re** was evaluated on several human cell lines, namely on tumoral – A2780 (epithelial ovarian cancer, cisplatin sensitive), A2780R (epithelial ovarian cancer, cisplatin resistant) and HeLa (epithelial cervical cancer), as well as on non-tumoral MRC-5 (fibroblast) cell lines (Table 2).

Initial studies were performed with incubation of the complexes for 48 h in the dark to compare their toxicity with a known chemotherapeutic drug, namely cisplatin. **LQ-Re** exhibited extremely low dark toxicity in all cell lines studied in this work. On the contrary, **Pt-LQ** was found to be the most cytotoxic complex in the dark with IC<sub>50</sub> values in the low micromolar range. The heterobimetallic **Pt-LQ-Re** complex exhibited moderate dark cytotoxicity against all cancer cell

**Table 1** Photophysical properties of the complexes at room temperature

Compound	Excitation <sup>a</sup> $\lambda_{\text{ex}}/\text{nm}$	Emission <sup>b</sup> $\lambda_{\text{em}}/\text{nm}$	Quantum yield <sup>b</sup> $\Phi_{\text{em}}/\%$	Lifetime $\tau/\text{ns}$	$^1\text{O}_2$ quantum yield ( $\Phi(^1\Delta_g)/\%$ PBS/acetonitrile)
<b>LQ-Re</b>	350	452, 575	0.28, 0.17	708	22/65
<b>Pt-LQ</b>	350	600	0.11	704	15/24
<b>Pt-LQ-Re</b>	350	449	0.14	509	11/19

<sup>a</sup> Measured in PBS solution. <sup>b</sup> Measured in DMSO, by comparison with the emission of  $[\text{Ru}(\text{bipy})_3]\text{Cl}_2$  in aerated water ( $\Phi_{\text{em}} = 0.040$ ).



**Table 2** IC<sub>50</sub> values (μM) and phototoxic index (PI)

	LQ-Re	Pt-LQ	Pt-LQ-Re	Cisplatin
<b>MRC-5 (non-tumoral)</b>				
48 h <sup>a</sup>	121 ± 10.1	14.3 ± 3.0	22.0 ± 5.3	8.4 ± 2.1
<b>A2780</b>				
48 h <sup>a</sup>	46.1 ± 6.5	9.1 ± 1.8	28.7 ± 4.2	1.7 ± 0.5
4 h <sup>b</sup>	145 ± 9.5	30.6 ± 5.5	124 ± 8.3	8.1 ± 2.4
4 h + irradiation <sup>c</sup>	7.8 ± 1.6	4.3 ± 0.8	18.4 ± 5.2	9.3 ± 2.1
PI	18.6	7.1	6.7	n.a. <sup>d</sup>
<b>A2780R</b>				
48 h <sup>a</sup>	198 ± 20.5	25.6 ± 4.6	27.8 ± 4.7	9.5 ± 2.3
4 h <sup>b</sup>	>200	55.6 ± 7.4	67.8 ± 10.6	28.9 ± 5.3
4 h + irradiation <sup>c</sup>	19.3 ± 2.1	7.5 ± 1.4	16.5 ± 2.7	27.5 ± 3.1
PI	>10	7.4	4.1	n.a. <sup>d</sup>
<b>HeLa</b>				
48 h <sup>a</sup>	155 ± 22	12.6 ± 4.6	42.8 ± 4.7	10.2 ± 2.3
4 h <sup>b</sup>	>200	34.8 ± 4.1	77.8 ± 8.4	32.4 ± 5.7
4 h + irradiation <sup>c</sup>	20.1 ± 6.5	5.5 ± 0.9	13.5 ± 4.1	35.2 ± 4.6
PI	>10	6.3	5.7	n.a. <sup>d</sup>

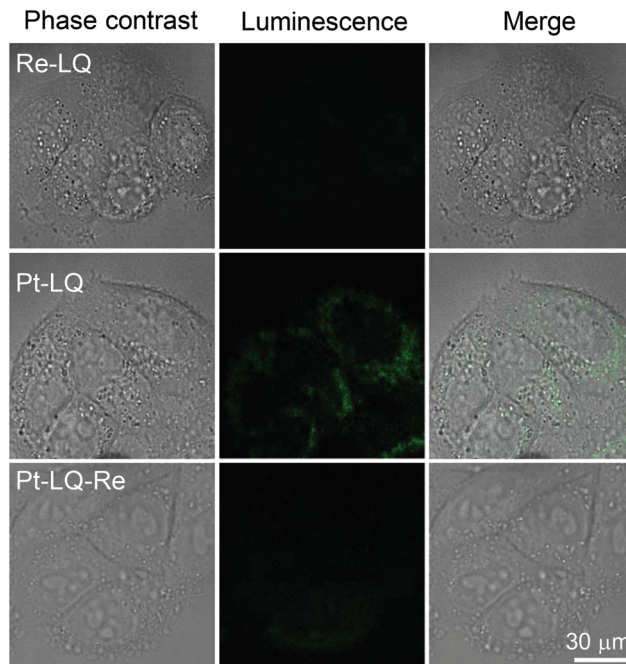
<sup>a</sup> 48 h incubation with complexes. <sup>b</sup> 4 h incubation with complexes and then 44 h incubation with fresh medium. <sup>c</sup> 4 h incubation with complexes, followed by 10 min irradiation at 350 nm (2.58 J cm<sup>-2</sup>) and then 44 h incubation with fresh medium. <sup>d</sup> Not applicable.

lines. Of note, all three complexes exhibited lower cytotoxicity than cisplatin on the non-tumoral MRC-5 cells. Unlike all other compounds, **Pt-LQ-Re** displayed a similar cytotoxic activity against the A2780 and A2780R cell lines, showing that this heterobimetallic complex can significantly circumvent cisplatin cross-resistance.

As anticipated, decreasing the exposure time of the cells to the complexes from 48 h to 4 h followed by 44 h incubation with fresh medium reduced significantly their cytotoxicity (Table 2, condition b). Upon light irradiation (350 nm, 2.58 J cm<sup>-2</sup>), **LQ-Re** exhibited the highest improvement in phototoxicity toward A2780 cancer cells with an interesting photo-index (PI) of 18.6, while a lower PI of 10 was observed on the A2780R and HeLa cell lines. These PI values are in agreement with the values reported by some of us for similar Re(i) tricarbonyl derivatives or with Photofrin.<sup>3,42</sup> Based on the singlet oxygen assay, one would expect that the **Pt-LQ-Re** complex should not exhibit significant phototoxicity in cancer cell lines. In line with this reasoning, the PI value of 6.7 presented by **Pt-LQ-Re** in the A2780 cell line is quite lower than the one displayed by **LQ-Re** (PI 18.6), although being comparable to the PI of **Pt-LQ**. In the other cell lines analyzed **Pt-LQ** and **Pt-LQ-Re** also display similar PI values.

### Cellular uptake and subcellular distribution

**Confocal microscopy.** The cellular uptake efficiency of each complex plays an important role in the cytotoxicity profile and needs to be taken into account to interpret the dark- and photo-toxicity data presented above. To visualize the cellular localization of the compounds in living cells, confocal fluorescence microscopy studies were performed. For this purpose, HeLa cells were incubated with the corresponding compounds (20 μM) for 2 h. As shown in Fig. 1, the signal of **LQ-Re** was too weak to be observed. It has been previously reported that the

**Fig. 1** Live fluorescence microscopy of HeLa cells treated with 20 μM of each compound for 2 h.

analogue complex having a 4-butylenic amine pendant arm instead of a 4-propylenic amine one, was observed exclusively in the cytoplasm, using however a much higher concentration (100 μM).<sup>36</sup>

Under the same experimental conditions as the one used for **LQ-Re**, **Pt-LQ-Re** homogeneously distributed throughout the cell, although the signal was still very weak. **Pt-LQ** was found to accumulate mostly in the cytoplasm. With the exception of **LQ-Re**, the confocal fluorescence imaging results are consistent with the results described below for the quantification of cellular uptake based on ICP-MS.

The non-visualization of the fluorescence signal of cellular accumulation of **LQ-Re** can be due to luminescence quenching processes that the compound undergoes once inside the cell, as reported for related Re(i) tricarbonyl complexes.<sup>43,38</sup> Our results reinforce the idea that for some luminescent compounds their true cellular accumulation and distribution can be distorted, as the intensity of the luminescence signal emitted from inside the cell can be depleted or enhanced upon interaction of the compounds with biological molecules that are present in the different cell compartments.

**Quantification of cellular uptake and subcellular distribution.** Cellular uptake studies in A2780 and A2780cisR cells were performed to evaluate the amount of **LQ-Re**, **Pt-LQ** and **Pt-LQ-Re** that enters into the cells and that localizes in the nucleus. The cells were incubated with complexes at 5 μM for 24 h and the cytoplasmic and nuclear fractions were isolated and analyzed by ICP-MS to quantify the presence of the corresponding metals (Pt and/or Re).

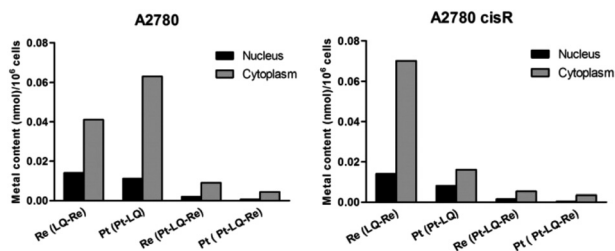


**Fig. 2** Subcellular distribution of LQ-Re, Pt-LQ and Pt-LQ-Re in A2780 cells and in A2780 cisR cells after 24 h of incubation with 5  $\mu$ M of each complex. Data are expressed as the metal (nmol Re or Pt) content in the nucleus or cytoplasm per million cells.

As can be seen in Fig. 2, the most striking difference is the much lower ability of **Pt-LQ-Re** to cross the cell membrane and to reach the cytoplasm and nuclear compartment if compared with **LQ-Re** and **Pt-LQ**. For the Pt-containing compounds, it can also be concluded from these results that the neutral complex **Pt-LQ** has a better cellular uptake than the positively charged complex **Pt-LQ-Re**. This agrees with the cytotoxicity assay, which showed that **Pt-LQ** exhibited the highest dark cytotoxicity of these two compounds. Most probably, the lower cellular uptake of the heterobimetallic complexes **Pt-LQ-Re** reflects its increased size and molecular weight, in comparison with the corresponding **LQ-Re** and **Pt-LQ** units.

**DNA interactions.** The experiments reported above have shown that our Pt-containing compounds (**Pt-LQ** and **Pt-LQ-Re**) are moderately cytotoxic to cancer cells and that irradiation enhances their activity. It is important to highlight that the Pt starting material itself (picolinic complex) is not cytotoxic,<sup>27</sup> although its oxidation to Pt(IV) afforded an active complex.<sup>44</sup> All in all, the functionalization of the Pt fragment with **LQ** seems to be a key factor in the cytotoxicity observed.

To gain the first insight into the mechanism of action of the new heterobimetallic Pt/Re complex, we have studied the binding effect of **Pt-LQ-Re** on DNA tertiary structure models. This was done by assessing its capacity to alter the electrophoretic mobility of the covalently closed circular (ccc) and open circular (oc) isoforms of a model plasmid such as pBR322. Pt<sup>II</sup> complexes and in particular cisplatin<sup>45</sup> have been widely reported to produce changes in both plasmid DNA isoforms: reducing the ccc mobility (*via* unwinding) and increasing the oc mobility until both reach a co-migration point.<sup>46</sup> Fig. 3 shows the results of the experiments performed with increasing amounts of **Pt-LQ-Re** and cisplatin (as a control) with the plasmid pBR322 simultaneously under two different conditions: (a) maintaining the samples at 37 °C in the dark; (b) irradiating the sample for 4 h at 350 nm (32.40 J cm<sup>-2</sup>) and then maintaining it in the dark at 37 °C.

In the dark, **Pt-LQ-Re**, contrary to cisplatin, does not alter the mobility of the plasmid. Cisplatin, on the other hand, altered both forms that finally co-migrate at  $r_i = 0.02$  ( $r_i$  = molar ratio Pt/nucleotide), as previously reported.<sup>45</sup>

After irradiation of **Pt-LQ-Re** for 30 min (4.05 J cm<sup>-2</sup>), 2 h (16.20 J cm<sup>-2</sup>) (data not shown) and 4 h (32.40 J cm<sup>-2</sup>), we

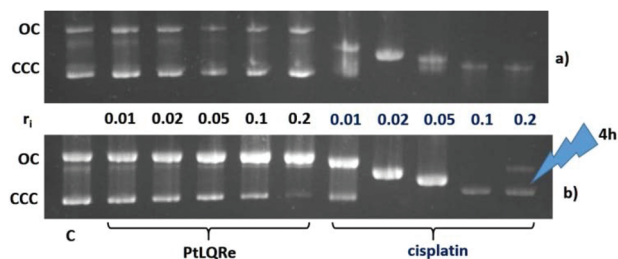


**Fig. 3** Agarose gel electrophoresis of the pBR322 plasmid treated with **Pt-LQ-Re** and cisplatin (a) in the dark and (b) after irradiation. For both gels lane 1 – C DNA plasmid control; lanes 2 to 6 – DNA incubated with **Pt-LQ-Re** at  $r_i$  0.01 to 0.2 and lanes 7 to 12 – DNA incubated with cisplatin at  $r_i$  0.01 to 0.2.  $r_i$  is the ratio of metal complex : DNA base pairs. OC – open circular and CCC covalently closed circular.

observed some differences in the mobility and amount of the plasmid DNA isoforms (lines 2 to 6). **Pt-LQ-Re** only slightly altered the mobility of the supercoiled form ccc (lines 3 to 5, experiment b), showing that DNA platination does not occur to an appreciable extent. However, the ccc isoform is almost fully converted to oc at the highest tested concentration (line 6,  $r_i = 0.2$ ). One likely explanation of this behavior is that upon light irradiation there is singlet oxygen production and relative oxidative damage, which leads to DNA single strand breaks (SSBs).

As can be clearly observed in the plasmid DNA interaction assay, upon light irradiation for higher concentrations, the supercoiled isoform of the plasmid was almost completely converted to the open circular isoform (Fig. 3). To characterize whether the *in vitro* oxidative damage to the DNA was also observed in living cells, we have also performed pulse field gel electrophoresis of A2780 cells treated with 20  $\mu$ M of **Pt-LQ-Re** in the dark and upon light irradiation at 350 nm for 10 min (2.58 J cm<sup>-2</sup>). It is possible to observe only negligible double strand breaks (DSBs) and no extended DNA fragmentation on A2780 cancer cells upon treatment with the target complex, confirming that the oxidative damage produced by **Pt-LQ-Re** on DNA leads mainly to single strand breaks (see Fig. S7†).

Moreover, it was not possible to detect any platination by ICP-MS analysis of the DNA extracted from the cells treated with **Pt-LQ-Re**, in the dark or under irradiation. This agrees with the results of the gel electrophoresis experiments and suggests once again that the cytotoxic effect of **Pt-LQ-Re** at the DNA level is related to its photosensitization and relative production of <sup>1</sup>O<sub>2</sub>.

**Biodistribution and imaging.** Finally, we have performed biodistribution and imaging studies of **Pt-LQ-Tc** in normal mice, to prove the theranostic capabilities of these types of heterobimetallic complexes. To perform these studies, **Pt-LQ-Tc** was injected into Balb/C mice. The animals were euthanized 1 h and 4 h after administration. Samples of blood and urine were collected and analyzed by radio-HPLC after adequate treatment, as detailed in the Experimental section, to gain a further insight into the **Pt-LQ-Tc** stability in the biological milieu. These studies revealed that the circulating radioactivity



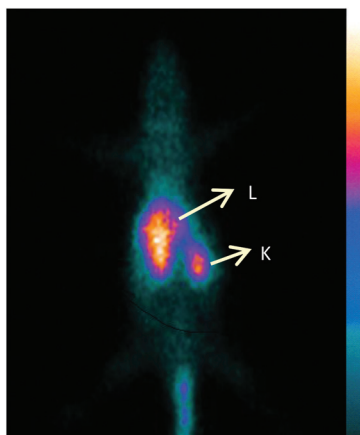


Fig. 4 Planar scintigraphic image of a Balb/C mouse injected with Pt-LQ-Tc at 1 h p.i. (L = liver; K = kidney).

in the serum corresponds mainly to intact **Pt-LQ-Tc** at least at 1 h post injection (p.i.) (Fig. S8†). This encouraging result points out that the congener **Pt-LQ-Re** might also have a favourable stability in the bloodstream. In contrast, one major metabolite was found in the urine in addition to intact **Pt-LQ-Tc** (Fig. S8†).

The biodistribution data obtained for **Pt-LQ-Tc**, at 1 h and 4 h p.i. times, are presented in the ESI (Table S1 and Fig. S9†). **Pt-LQ-Tc** has a slow clearance from the blood stream ( $3.9 \pm 1.0\%$  ID  $\text{g}^{-1}$ , 4 h p.i.) with an important uptake in excretory organs (liver and kidney). The lipophilic nature of this radioactive heterobimetallic compound justifies its very slow excretion, involving most probably the hepatobiliary route. In particular, the accumulation of radioactivity in the stomach is rather low (<2% per organ) showing that the  $^{99\text{m}}\text{Tc}$  core of this heterobimetallic Pt(II)/Tc(I) compound resists *in vivo* oxidation towards pertechnetate. The biodistribution properties of **Pt-LQ-Tc** were further corroborated by imaging studies that allowed a clear visualization of the accumulation of radioactivity in the excretory organs, namely liver and kidney, as shown in Fig. 4.

## Conclusions

The development of novel anticancer agents with imaging, chemotherapeutic and photosensitizing properties within a single molecule is highly sought. In this article, we demonstrated that a new heterobimetallic complex containing platinum and rhenium (**Pt-LQ-Re**) had indeed photosensitizing properties due to the presence of a rhenium core and an intrinsic cytotoxic activity in the dark due to the presence of a non-classical platinum core. Importantly, it could be shown that the Re tricarbonyl unit in **Pt-LQ-Re** could be replaced by  $^{99\text{m}}\text{Tc}$  to allow for *in vivo* imaging and, moreover, that the “cold” complex could overcome cisplatin-resistance. Overall, the biological results of this study are quite appealing, justifying further studies for a better understanding of the biological

effects induced by this new class of heterobimetallic complexes.

## Experimental section

### General procedures

All chemicals and solvents were of reagent grade and were used without purification unless stated otherwise. Solvents were dried and distilled prior to use according to the described procedures.<sup>47</sup> Unless stated otherwise, the syntheses of the ligands and complexes were not carried out under a nitrogen atmosphere, or using standard Schlenk techniques and dry solvents; the work-up procedures were all performed in air. The platinum complex *trans*-[PtCl<sub>2</sub>(4-picolinic acid)(isopropylamine)] and the starting material *fac*-[Re(CO)<sub>3</sub>(H<sub>2</sub>O)<sub>3</sub>]Br were synthesized as described elsewhere.<sup>27,29</sup> Na[ $^{99\text{m}}\text{TcO}_4$ ] was eluted from a commercial  $^{99}\text{Mo}/^{99\text{m}}\text{Tc}$  generator, using a 0.9% saline solution.

$^1\text{H}$  and  $^{13}\text{C}$  NMR spectra were recorded on a Varian Unity 300 MHz and a Bruker DRX 500 spectrometer, and  $^{195}\text{Pt}$  NMR spectra were recorded on a Varian Unity 500 MHz and a Bruker Advance II-HD Nanobay 300 spectrometer;  $^1\text{H}$  and  $^{13}\text{C}$  chemical shifts are given in ppm and were referenced to the residual solvent resonances relative to SiMe<sub>4</sub>.  $^{195}\text{Pt}$  chemical shifts were assigned using a solution of K<sub>2</sub>[PtCl<sub>4</sub>] in saturated aqueous KCl as the external reference. The shift for K<sub>2</sub>PtCl<sub>4</sub> was adjusted to −1628 ppm from Na<sub>2</sub>PtCl<sub>6</sub> ( $\delta = 0$  ppm). The NMR samples were prepared in CDCl<sub>3</sub> or CD<sub>3</sub>OD. The spectra were assigned with the help of 2D experiments ( $^1\text{H}$ – $^1\text{H}$  correlation spectroscopy, and  $^1\text{H}$ – $^{13}\text{C}$  heteronuclear single quantum coherence). The spectra recorded for the monitoring of the **Pt-LQ-Re** reaction with GMP were obtained in D<sub>2</sub>O : MeOD (3 : 1) using trimethylsilyl propanoic acid as an internal reference.

IR spectra were recorded in the range 4000–400  $\text{cm}^{-1}$  as KBr or CsI pellets on a Bruker Tensor 27 spectrometer. Electrospray ionization mass spectrometry (ESI-MS) was performed using a Bruker HCT electrospray ionization quadrupole ion trap mass spectrometer.

Thin layer chromatography (TLC) was performed on Merck silica gel 60 F254 plates. Column chromatography was performed with silica gel 60 (Merck). Radioactivity measurements were performed using an ionization chamber Aloka, Curiometer IGC-3 or a  $\gamma$ -counter Berthold, LB 2111. HPLC analysis of the ligands, Re, Pt and  $^{99\text{m}}\text{Tc}$  complexes, was performed on a Perkin-Elmer LC pump 200 coupled to a LC 290 tunable UV-vis detector and to a Berthold LB-507A radiometric detector, using an analytic Supelco Discovery C18 reversed-phase column with a pre-column, 25 cm  $\times$  4.6 mm, 5  $\mu\text{m}$ , with a flow rate of 1  $\text{mL min}^{-1}$ ; UV detection, 254 nm. HPLC purification of the Re and Pt complexes was performed in a HPLC system of Waters 2535 Quaternary Gradient, using a semi-preparative Supelco C18 reversed-phase column, 25 cm  $\times$  10 mm, 10  $\mu\text{m}$ , with a flow rate of 2  $\text{mL min}^{-1}$ . Eluents: aqueous 0.9% NaCl solution, B: MeOH. The HPLC analysis was performed with gradient elution, using the following methods:

**Method 1.** 0–3 min, 100% A; 3–3.1 min, 100%–75% A; 3.1–9 min, 75% A; 9–9.1 min 75%–66% A; 9.1–20 min, 66%–0% A; 20–25 min, 0% A; 25–25.1 min, 0%–100% A; 25.1–30 min, 100% A.

**Method 2.** 0–3 min, 100% A; 3–3.1 min, 100%–75% A; 3.1–9 min, 75% A; 9–9.1 min 75%–66% A; 9.1–15 min, 66%–0% A; 15–25 min, 0% A; 25–25.1 min, 0%–100% A; 25.1–30 min, 100% A.

**Method 3.** 0–3 min, 100% A; 3–3.1 min, 100%–75% A; 3.1–9 min, 75% A; 9–9.1 min 75%–66% A; 9.1–20 min, 66%–0% A; 20–30 min, 0% A; 30–30.1 min, 0%–100% A; 30.1–35 min, 100% A.

**Method 4.** 0–3 min, 100% A; 3–3.1 min, 100%–75% A; 3.1–9 min, 75% A; 9–9.1 min 75%–66% A; 9.1–24 min, 66%–0% A; 24–29 min, 0% A; 29–29.1 min, 0%–100% A; 29.1–30 min, 100% A.

### Synthesis and characterization of chelators, Re(i) and Pt(II) complexes

**Synthesis of *tert*-butyl-3-(bis(quinolin-2-ylmethyl)amino)propylcarbamate (LQ-Boc).** A solution of 2-quinolinecarboxaldehyde (189 mg, 1.200 mmol) in dichloroethane (2.0 mL, DCE) was added at 0 °C, under nitrogen, to a solution of *N*-Boc-1,3-propanediamine (0.1 mL, 0.570 mmol) and Na(OAc)<sub>3</sub>BH (302 mg, 1.430 mmol) in DCE (6.0 mL). The mixture was stirred at room temperature for 4 h. After evaporation of DCE, the reaction mixture was quenched with water and extracted with chloroform. The combined organic phases were dried over Na<sub>2</sub>SO<sub>4</sub>, concentrated under reduced pressure and purified through a pad of silica gel (eluent: CHCl<sub>3</sub> (100–95%)/MeOH (0–5%)). **LQ-Boc** was obtained as a dark orange oil after removal of the solvent from the collected fractions (111 mg, 0.240 mmol,  $\eta$  = 42%).

$R_f$  (10% MeOH/DCM) = 0.29;  $R_{\text{time}}$ -HPLC (Method 1) = 22.0 min; <sup>1</sup>H-NMR (300 MHz, CDCl<sub>3</sub>):  $\delta$  = 1.38 (s, 9H, Boc); 1.76 (m, 2H, H-2); 2.72 (t, 2H, H-3); 3.18 (m, 2H, H-1); 4.00 (s, 4H, H-4); 5.78 (br s, 1H, NH-Boc); 7.50 (dd, 2H, Ar); 7.66 (dd, 4H, Ar); 7.77 (d, 2H, Ar); 8.10 (dd, 4H, Ar); <sup>13</sup>C-NMR (300 MHz, CDCl<sub>3</sub>):  $\delta$  = 29.42 (3 CH<sub>3</sub>-Boc); 30.27 (C-2); 39.81 (C-1); 53.40 (C-3); 61.57 (C-4); 79.33 (Cq-Boc); 121.78 (CH-Arom); 126.95 (CH-Arom); 127.96 (Cq-Arom); 128.11 (CH-Arom); 128.45 (Cq-Arom); 129.59 (CH-Arom); 130.14 (CH-Arom); 137.23 (CH-Arom); 148.06 (C=O Boc); 156.67 (Cq-Arom); ESI-MS (+) C<sub>28</sub>H<sub>32</sub>N<sub>4</sub>O<sub>2</sub> (456.3) ( $m/z$ ) (%): 457.3 [M + H]<sup>+</sup> (100), 479.3 [M + Na]<sup>+</sup> (29).

**Synthesis of *N,N'*-bis(quinolin-2-ylmethyl)propane-1,3-diamine (LQ).** **LQ-Boc** (179 mg, 0.380 mmol) was dissolved in MeOH (12.0 mL), and HCl 37% (2.1 mL) was added, at 0 °C, dropwise. The mixture was stirred at room temperature for 24 h. The pH was adjusted to 10–12 with aqueous NaOH. After evaporation of the MeOH under reduced pressure, the mixture was extracted with chloroform. The combined organic phases were dried over Na<sub>2</sub>SO<sub>4</sub> and concentrated under reduced pressure to give **LQ** as a brown oil (131.0 mg, 0.370 mmol,  $\eta$  = 97%).

$R_f$  (100% MeOH) = 0.13;  $R_t$ -HPLC (Method 1) = 18.0 min; <sup>1</sup>H-NMR (300 MHz, CDCl<sub>3</sub>):  $\delta$  = 1.74 (m, 2H, H-2); 2.69 (t, 2H, H-3); 2.76 (t, 2H, H-1); 4.01 (s, 4H, H-4); 7.57 (dd, 2H, Ar); 7.69 (dd, 4H, Ar); 7.76 (d, 2H, Ar); 8.12 (dd, 4H, Ar); <sup>13</sup>C-NMR (300 MHz, CDCl<sub>3</sub>):  $\delta$  = 29.89 (C-2); 40.07 (C-1); 52.25 (C-3); 61.38 (C-4); 121.07 (CH-Arom); 126.31 (CH-Arom); 127.36 (Cq-Arom); 127.59 (CH-Arom); 128.98 (CH-Arom); 129.53 (CH-Arom); 136.61 (CH-Arom); 147.58 (Cq-Arom); 160.33 (Cq-Arom); ESI-MS (+) C<sub>23</sub>H<sub>24</sub>N<sub>4</sub> (356.5) ( $m/z$ ) (%): 357.4 [M + H]<sup>+</sup> (100).

### Synthesis of the Re complex of *N,N'*-bis(quinolin-2-ylmethyl)propane-1,3-diamine ([LQ-Re]X, X = Cl, Br)

**LQ-Re** was synthesized by two different approaches (method A and method B), as described below.

**Method A (X = Br):** To a solution of **LQ** (123 mg, 0.350 mmol) in MeOH (22.0 mL) was added [Re(CO)<sub>3</sub>(H<sub>2</sub>O)<sub>3</sub>]Br (143 mg, 0.350 mmol) and the resulting solution was refluxed overnight. After solvent evaporation, the solid obtained was washed with water, redissolved in MeOH and centrifuged at 4000 rpm for 10 minutes. The solid was discarded and the liquid was dried under reduced pressure. The residue was then washed with diethyl ether and chloroform, to give **LQ-Re** as a dark orange oil (182 mg, 0.290 mmol,  $\eta$  = 83%).

**Method B (X = Cl):** To a solution of **LQ** (50 mg, 0.140 mmol) in THF (10.0 mL) was added Re(CO)<sub>5</sub>Cl (51 mg, 0.140 mmol) and refluxed overnight. After this time, the solvent was removed under reduced pressure and the desired product was purified by semipreparative HPLC (Method 2) to give a dark orange oil (60 mg, 0.096 mmol,  $\eta$  = 69%).

$R_t$ -HPLC (Method 2) = 26.6 min; <sup>1</sup>H-NMR (300 MHz, MeOD + CDCl<sub>3</sub>):  $\delta$  = 2.49 (m, 2H, H-2); 3.21 (t, 2H, H-1); 4.07 (dd, 2H, H-3); 5.32 (dd, 4H, H-4); 7.74 (dd, 4H, Ar); 7.91 (dd, 2H, Ar); 8.05 (d, 2H, Ar); 8.56 (dd, 4H, Ar); <sup>13</sup>C-NMR (300 MHz, MeOD + CDCl<sub>3</sub>):  $\delta$  = 25.06 (C-2); 37.92 (C-1); 65.49 (C-3); 69.53 (C-4); 120.78 (CH-Arom); 129.24 (CH-Arom); 129.33 (CH-Arom); 129.56 (Cq-Arom); 130.77 (CH-Arom); 134.03 (CH-Arom); 142.86 (CH-Arom); 147.98 (Cq-Arom); 165.78 (Cq-Arom); 195.20 (2 × C=O); 196.79 (C=O); ESI-MS (+) C<sub>26</sub>H<sub>24</sub>N<sub>4</sub>O<sub>3</sub>Re (627.70) ( $m/z$ ) (%): 627.30 (100), 625.3 (67), 628.3 (35), 626.3 (11), 629.3 (6); IR  $\nu_{\text{max}}$ (CsI)/cm<sup>−1</sup> (C=O) 2018, 1897.

### Synthesis of mono((4-(3-(bis(quinolin-2-ylmethyl)amino)propylcarbamoyl)pyridinium-1-yl)(isopropylammonio)platinum(II) dichloride (Pt-LQ)

*N*-Hydroxysuccinimide (17 mg, 0.130 mmol) was added to a solution of *t*-[PtCl<sub>2</sub>(4-picolinic acid)(isopropylamine)] (47 mg, 0.110 mmol) in DCM (14.0 mL). The solution was stirred for 15 minutes, and then 1-ethyl-3-(3-dimethylaminopropyl)carbodiimide (26 mg, 0.130 mmol) was added. After stirring for 16 h at room temperature, the solution was evaporated to dryness and 5 mL of water were added. The resulting mixture was filtered to separate the urea by-product and the resulting mixture was evaporated to dryness. The activated ester was redissolved in dry DMF (3.5 mL), and added to a solution of **LQ** (75 mg, 0.210 mmol), DIPEA (the minimal volume to reach

pH > 8) and dry DMF (6.0 mL). The reaction mixture was stirred for 22 h, under a nitrogen atmosphere, at room temperature.

After solvent evaporation, the remaining oil was purified by semi-preparative HPLC (Method 3); the collected fraction was dried under vacuum to give **Pt-LQ** as an orange oil (49 mg, 0.062 mmol,  $\eta$  = 58%).

**R<sub>f</sub>-HPLC** (Method 1) = 21.3 min; **<sup>1</sup>H-NMR** (300 MHz, MeOD):  $\delta$  = 1.39 (d, 6H, H-6); 1.93 (m, 2H, H-2); 2.73 (t, 2H, H-3); 3.39 (m, 1H, H-5); 3.46 (t, 2H, H-1); 4.04 (s, 4H, H-4); 7.37 (d, 2H, H-8); 7.60 (dd, 2H, Ar); 7.74 (dd, 4H, Ar); 7.85 (d, 2H, Ar); 7.95 (d, 2H, Ar); 8.22 (d, 2H, Ar); 8.75 (d, 2H, H-7); **<sup>13</sup>C-NMR** (300 MHz, MeOD):  $\delta$  = 23.78 (C-6); 26.57 (C-2); 38.40 (C-1); 49.42 (C-5); 52.48 (C-3); 61.75 (C-4); 122.31 (CH-Arom); 123.33 (C-8); 127.90 (CH-Arom); 128.56 (CH-Arom); 128.79 (Cq); 129.00 (CH-Arom); 131.00 (Cq); 131.14 (CH-Arom); 138.69 (CH-Arom); 148.04 (Cq); 149.18 (C=O); 153.90 (C-7); 161.60 (Cq); **<sup>195</sup>Pt-NMR** (400 MHz, MeOD):  $\delta$  = -2098.39; **ESI-MS** (+) C<sub>32</sub>H<sub>36</sub>Cl<sub>2</sub>N<sub>6</sub>O<sub>4</sub>Pt (786.20) (*m/z*) (%): 787.3 (100), 786.5 (77), 788.2 (70), 789.2 (63), 785.6 (57), 790.2 (21), 791.1 (15), 792.1 (4); **IR**  $\nu_{\max}$ (KBr)/cm<sup>-1</sup> (CO) 1643; (NH) 3429.

#### Synthesis of the Re complex of mono ((4-(3-(bis(quinolin-2-ylmethyl)amino)propylcarbamoyl)pyridinium-1-yl) (isopropylammonio)platinum(II) dichloride (**Pt-LQ-Re**)

**Pt-LQ-Re** was synthesized by two different approaches (method A and method B), as described below.

**Method A:** *N*-Hydroxysuccinimide (13 mg, 0.090 mmol) was added to a solution of *t*-[PtCl<sub>2</sub>(4-picolinic acid)(isopropylamine)] (35 mg, 0.080 mmol) in DCM (10.0 mL). The solution was stirred for 15 minutes, and then 1-ethyl-3-(3-dimethylaminopropyl)carbodiimide (19 mg, 0.090 mmol) was added. After stirring for 16 h at room temperature, the solution was evaporated to dryness and 5 mL of water were added. The resulting mixture was filtered to separate the urea by-product and the resulting mixture was evaporated to dryness. The activated ester was redissolved in dry DMF (3.0 mL), and added to a solution of [**LQ-Re**]Cl (53 mg, 0.080 mmol) and DIPEA (the minimal volume to reach pH > 8) in dry DMF (5.0 mL). The reaction mixture was stirred overnight at room temperature.

After solvent evaporation, the remaining oil was purified by semi-preparative HPLC (Method 3), and the collected fraction was dried under vacuum to give **Pt-LQ-Re** as a light orange oil (16 mg, 0.015 mmol,  $\eta$  = 19%).

**Method B:** To a solution of **Pt-LQ** (30 mg, 0.038 mmol) in THF (6.0 mL) was added [Re(CO)<sub>5</sub>Cl] (14 mg, 0.038 mmol) and the resulting solution was refluxed overnight. After this time, the solvent was removed under reduced pressure and the desired product was purified by HPLC (Method 3) to give a light orange oil (11 mg, 0.011 mmol,  $\eta$  = 29%).

**R<sub>f</sub>-HPLC** (Method 2) = 25.3 min; **<sup>1</sup>H-NMR** (300 MHz, MeOD):  $\delta$  = 1.43 (d, 6H, H-6); 2.44 (m, 2H, H-2); 3.57 (m, 1H, H-5); 3.69 (t, 2H, H-1); 4.06 (dd, 2H, H-3); 5.24 (dd, 4H, H-4); 7.65 (d, 2H, Ar); 7.76 (m, 4H, Ar + H-8); 7.92 (dd, 2H, Ar); 8.07 (d, 2H, Ar); 8.57 (dd, 4H, Ar); 8.98 (d, 2H, H-7); **<sup>13</sup>C-NMR** (300 MHz, MeOD):  $\delta$  = 23.90 (C-6); 27.17 (C-2); 38.60 (C-1); 47.83 (C-5); 67.03 (C-3); 69.85 (C-4); 120.81 (CH-Arom); 124.04

(C-8); 129.51 (2× CH-Arom); 129.87 (CH-Arom); 131.04 (2× Cq); 134.14 (CH-Arom); 143.01 (CH-Arom); 144.24 (Cq); 148.25 (C=O pic); 154.97 (C-7); 166.29 (Cq); 193.36 (C=O); 195.01 (2× C=O); **<sup>195</sup>Pt-NMR** (400 MHz, MeOD):  $\delta$  = -2098.20; **ESI-MS** (+) C<sub>35</sub>H<sub>36</sub>Cl<sub>2</sub>N<sub>6</sub>O<sub>4</sub>PtRe (1056.89) (*m/z*) (%): 1057.1 (100), 1056.3 (73), 1058.1 (62), 1059.1 (57), 1055.4 (55), 1060.1 (21), 1053.7 (16); **IR**  $\nu_{\max}$ (KBr)/cm<sup>-1</sup> (C=O) 1675; (C=O) 1975, 2025; (NH) 3450.

#### Synthesis and *in vitro* evaluation of the <sup>99m</sup>Tc complexes: **LQ-Tc** and **Pt-LQ-Tc**

**Synthesis.** The radioactive precursor *fac*-[<sup>99m</sup>Tc(CO)<sub>3</sub>(H<sub>2</sub>O)<sub>3</sub>]<sup>+</sup> was prepared by addition of 3 mL of Na[<sup>99m</sup>TcO<sub>4</sub>] to a mixture of potassium boranocarbonate (5 mg), sodium tartrate (7 mg) and sodium tetraborate (7 mg). After heating at 100 °C for 30 min, the pH was adjusted to 5. Then, in a nitrogen-purged glass vial, 0.8 mL of *fac*-[<sup>99m</sup>Tc(CO)<sub>3</sub>(H<sub>2</sub>O)<sub>3</sub>]<sup>+</sup> was added to 0.8 mL of an ethanolic solution of the compounds **Pt-LQ** (10<sup>-3</sup> M) or **Pt-LQ** (10<sup>-2</sup> M). The reaction mixtures were then heated for 60 min at 50 °C. After cooling to room temperature, prior to their *in vitro* evaluation, the <sup>99m</sup>Tc complexes were subjected to HPLC purification using a Supelco Discovery RP-column, using a gradient elution (Method 4) with a flow rate of 1 mL min<sup>-1</sup>. The solvent from the collected fractions was evaporated under a stream of nitrogen and the residue was redissolved in 0.9% NaCl to obtain the desired radioactive concentration. The purified complexes were analyzed by RP-HPLC and their chemical identity was ascertained by HPLC co-injection with the Re counterparts.

**R<sub>f</sub>-HPLC** (Method 4): **LQ-Tc**, 19.3 min; **Pt-LQ-Tc**, 26.4 min.

**Partition coefficient measurements.** The log *P*<sub>o/w</sub> values of the <sup>99m</sup>Tc complexes were determined by the “shake flask” method.<sup>48</sup> A mixture of octanol (1.0 mL) and 0.1 M PBS pH = 7.4 (1.0 mL) was stirred vigorously, followed by the addition of 25  $\mu$ L of the aqueous solutions of each complex. The mixtures were vortexed and centrifuged (3000 rpm, 10 min, RT) to allow phase separation. Aliquots of 25  $\mu$ L of the octanol and PBS phases were counted in a gamma counter. The partition coefficient (*P*<sub>o/w</sub>) was calculated by dividing the number of counts of the octanol phase by those from the PBS phase, and the results are expressed as log *D*<sub>o/w</sub>.

***In vitro* stability assays.** Aliquots (0.1 mL) of **Pt-LQ-Tc** solutions were added to 1 mL of the different challenging media (0.1 M PBS, pH 7.4; human serum; cell culture medium) and incubated at 37 °C for 2, 4, 6 and 24 h, except in the case of cell culture medium where the incubation was performed only for 4 h. After incubation, 0.4 mL aliquots of the human serum and cell culture medium mixtures were treated with 0.8 mL of EtOH to precipitate the proteins. The samples were centrifuged at 3000 rpm for 5 min, and the aliquots of the supernatant were analyzed by RP-HPLC. For the challenging experiment in PBS, the aliquots of the reaction mixture were directly injected in the HPLC without any treatment.

#### Photophysical measurements

**UV/Vis absorption spectra.** UV/Vis absorption spectra and extinction coefficients were obtained on a Varian Cary 50 Scan



UV/vis spectrophotometer using standard quartz cells with 1 cm path length.

**Emission spectra.** Emission spectra were recorded on an Edinburgh Instrument FLSP920 spectrometer equipped with a 450 W xenon lamp, double monochromators for the excitation and emission pathways, and a red-sensitive photomultiplier (PMT-R928) as a detector. The emission spectra were fully corrected by using the standard corrections supplied by the manufacturer for the spectral power of the excitation source and the sensitivity of the detector.

**Quantum yields.** The quantum yields were measured by use of an integrating sphere with an Edinburgh Instrument FLSP920 spectrometer. The absorbance of the samples was kept below 0.1 to avoid inner filter effects, except for the concentration-dependent measurements, and all measurements were carried out at 293 K.

**Luminescence lifetime.** The luminescence lifetimes were measured by using a  $\mu$ F900 pulse 60 W xenon microsecond flash lamp with a repetition rate of 100 Hz and a multi-channel scaling module. The emission was collected at right angles to the excitation source with the emission wavelength selected by using a double grating monochromator and detected by a R928-P PMT. The instrument response function (IRF) was measured by using the blank solvent as the scattering sample and setting the monochromator at the emission wavelength of the excitation beam. The resulting intensity decay is a convolution of the luminescence decay with the IRF and iterative convolution of the IRF with a decay function and non-linear least-squares analysis was used to analyze the convoluted data.

**Indirect evaluation of singlet oxygen.**<sup>49</sup> An air-saturated acetonitrile solution containing the complex (OD = 0.1 at irradiation wavelength), *p*-nitrosodimethyl aniline (RNO, 24  $\mu$ M), and imidazole (12 mM) or an air-saturated PBS buffer solution containing the complex (OD = 0.1 at irradiation wavelength), RNO (20  $\mu$ M), and histidine (10 mM) was irradiated in a luminescence quartz cuvette at 350 or 420 nm in a RPR100 Rayonet chamber reactor (Southern New England Ultraviolet Company) complete with six lamps, at different time intervals. The absorbance of the solution was then evaluated. The plots of variations in absorbance at 440 nm in PBS or at 420 nm in acetonitrile ( $A_0 - A$ , where  $A_0$  is the absorbance before irradiation) versus the irradiation times for each sample were prepared and the slope of the linear regression was calculated ( $S_{\text{sample}}$ ). As a reference compound, phenalenone ( $\Phi_{\text{ref}}(^1\text{O}_2) = 95\%$ ) was used in both methods, to obtain  $S_{\text{ref}}$  eqn (1) was applied to calculate the singlet oxygen quantum yields ( $\Phi_{\text{sample}}$ ) for every sample:

$$\Phi_{\text{sample}} = \Phi_{\text{ref}} \times S_{\text{sample}} / S_{\text{ref}} \times I_{\text{ref}} / I_{\text{sample}} \quad (1)$$

$$I = I_0 \times (1 - 10^{-A_\lambda}) \quad (2)$$

$I$  (absorbance correction factor) was obtained with eqn (2), where  $I_0$  is the light intensity of the irradiation source in the

irradiation interval and  $A_\lambda$  is the absorbance of the sample at wavelength  $\lambda$ .

## Cellular studies

**Cell culture.** Human ovarian epithelial cancer A2780 (cis-platin sensitive) and A2780R (acquired cisplatin resistance) cell lines were maintained in RPMI1640 medium. Human cervical carcinoma cells (HeLa) were grown in DMEM containing GlutaMax I and the normal lung fibroblast cell line (MRC-5) was cultured in F-10 medium. All culture media were supplemented with 10% heat-inactivated foetal bovine serum (FBS) and 1% penicillin/streptomycin antibiotic solution. All culture media and supplements were from Gibco.

**Dark- and photo-toxicity.** A fluorometric cell viability assay using resazurin (Promocell GmbH) was used to compare the cytotoxicity of the complexes in the dark and upon UV irradiation. A2780 and A2780R cell lines were plated in triplicates in 96-well plates at a density of 4000 cells per well in 100  $\mu$ L, whereas the MRC-5 cell line was plated in triplicates in 96-well plates at a density of 7500 cells per well in 100  $\mu$ L, 24 h prior to treatment. The cells were then treated with increasing concentrations of compounds for 48 h. For phototoxicity studies, the cells were treated for 4 h with increasing concentrations of the compounds in the dark. After that, the medium was removed and replaced by fresh culture medium prior to 10 min irradiation at 350 nm ( $2.58 \text{ J cm}^{-2}$ ). After 44 h in the incubator, the medium was replaced by 100 mL complete medium containing resazurin (final concentration  $0.2 \text{ mg mL}^{-1}$ ). After 4 h incubation at 37  $^\circ\text{C}$ , fluorescence of the highly red fluorescent resorufin product was quantified at 590 nm emission with 540 nm excitation wavelength in a SpectraMax M5 microplate reader. Light doses were evaluated with a Gigahertz Optic X1-1 optometer.

**Cellular uptake and distribution by ICP-MS.** To assess the uptake of complexes and their intracellular distribution, A2780 and A2780cisR cells were exposed to the complexes and the Pt and Re content in the nucleus and cytoplasm was analyzed by ICP-MS.

The cells were seeded into 24-well tissue culture plates at a density of 200 000 and 400 000 cells for A2780 and A2780cisR, respectively, and allowed to attach overnight at 37  $^\circ\text{C}$ . The adherent cells were incubated with each complex (5  $\mu$ M) for 24 h at 37  $^\circ\text{C}$ . Then, the cells were washed with PBS and detached from plates with trypsin. In suspension, the cells were counted, washed twice with cold PBS, and centrifuged (800 rpm, 2 min, 4  $^\circ\text{C}$ ) to obtain a pellet. In order to disrupt the cellular membrane, the pellet was resuspended in lysis buffer (10 mM Tris, 1.5 mM  $\text{MgCl}_2$ , 140 mM NaCl, pH 8.0–8.3) with a Nonidet P40 (0.02%). After 15 min incubation on ice, the suspension was centrifuged at 1300g for 2 min at 4  $^\circ\text{C}$  and the nuclear fraction (pellet) was separated from the cytoplasmic fraction (supernatant).

The Pt content for complexes **Pt-LQ** and **Pt-LQ-Re** and the Re content for complexes **LQ-Re** and **Pt-LQ-Re**, in the two fractions, were measured by ICP-MS. The measurements were per-

formed after digestion with ultrapure  $\text{HNO}_3$  (65%),  $\text{H}_2\text{O}_2$  and  $\text{HCl}$ , followed by evaporation and redissolution of the residue in ultrapure water to obtain a 2.0% (v/v) nitric acid solution, using a ICP-MS NexION 300xx PerkinElmer instrument and  $^{187}\text{Rhenium}$  as an internal standard.

**Confocal fluorescence microscopy studies.** Cellular localization of the compounds was also assessed by fluorescence microscopy using HeLa cells. The cells were grown on 35 mm Cellview glass bottom dishes (Greiner) in 3 mL complete medium at a density of  $1 \times 10^5$  cells per mL and incubated for 2 h with the complexes at a concentration of 20  $\mu\text{M}$ . The cells were washed with  $1 \times$  PBS prior to imaging by confocal microscopy using a CLSM Leica SP5 Mid UV-VIS Leica microscope. All the complexes were excited at 355 nm and the emission above 420 nm was recorded.

### Animal studies

**Biodistribution and imaging studies.** All animal experiments were performed in compliance with Portuguese regulations for animal treatment. The animals were housed in a temperature- and humidity-controlled room with a 12 h light/12 h dark schedule. Biodistribution of the radiocomplex was estimated in healthy Balb/C mice (8–10 weeks old). Animals were intravenously injected with the radiolabelled complex (3–10 MBq) diluted in 100  $\mu\text{L}$  of PBS pH 7.2 into the retro-orbital sinus. Mice were sacrificed by cervical dislocation at 1 h and 4 h post-injection (p.i.). The administered dose and the radioactivity in the sacrificed animals were measured in a dose calibrator (Aloka, Curiometer IGC-3, Tokyo, Japan or Capintec CRC-15 W, Ramsey, USA). The difference between the radioactivity in the injected and sacrificed animals was assumed to be due to excretion. Tissues of interest were dissected, rinsed to remove excess blood, weighed, and their radioactivity was measured using a gamma counter (Berthold, LB2111, Germany). The uptake in the tissues of interest was calculated and expressed as a percentage of the injected radioactivity dose per gram of tissue (% ID  $\text{g}^{-1}$ ). For blood, bone, muscle and skin, the total activity was estimated assuming that these organs constitute 6%, 10%, 40% and 15% of the total body weight, respectively. Urine was also collected and pooled together at the time of sacrifice.

For imaging, the animals were injected with **Pt-LQ-Tc** (5 MBq) into the tail vein and sacrificed at 1 h p.i. A set of static images ( $256 \times 256$  matrix, Zoom 2, 2 min) was acquired, by placing the animals over a  $\gamma$ -camera (GE 400AC; Maxicamera, Milwaukee, USA) coupled with a high-resolution parallel collimator and controlled with the GENIE Acquisition computer.

**In vivo stability.** The *in vivo* stability of **Pt-LQ-Tc** was evaluated in urine and serum by HPLC analysis, using method 4, at 1 h (p.i.). The urine was collected at the time of sacrifice and analyzed by HPLC. Blood was collected from mice and immediately centrifuged for 5 min at 3000 rpm, and the serum was separated. Aliquots of 0.1 mL of serum were treated with 0.2 mL of EtOH to precipitate the proteins. The samples were centrifuged at 3000 rpm, for 10 min, and the supernatant was collected and analyzed by RP-HPLC.

### DNA interaction studies

**Plasmid DNA interaction studies.** The DNA interaction studies were performed in a total volume of 20  $\mu\text{L}$ . The DNA stock was purchased to Gencust at a concentration of 0.5  $\mu\text{g } \mu\text{L}^{-1}$  in phosphate buffer 50 mM (pH = 7.4). Stock solutions of the complexes were prepared in DMSO at 5 mM. The 20  $\mu\text{L}$  samples containing 0.125  $\mu\text{g } \mu\text{L}^{-1}$  of DNA-pBR322 in 10 mM Tris-HCl (pH 7.6) and 1 mM EDTA were incubated with the platinum compounds at *ri* values ranging from 0.05 to 0.2 (defined as the molar ratio of Pt/nucleotide). The samples were incubated simultaneously in the dark and with light at 350 nm for 4 h ( $32.4 \text{ J cm}^{-2}$ ) and afterwards all together in the dark and 37  $^\circ\text{C}$  in a thermoshaker for 24 h. After the incubation 2  $\mu\text{L}$  of a loading dye containing 50% glycerol, 0.25% bromophenol blue and 0.25% xylene cyanol was added. The total content of the sample was loaded in the agarose gel (1.2% p/v) and electrophoresis was carried out for a period of 150 min, approximately at 70 V in a TAE  $1 \times$  (Tris-acetate/EDTA) buffer. After electrophoresis, the gel was immersed in 200 mL of Millipore water containing 10 mL from a 10  $\text{mg mL}^{-1}$  stock solution of ethidium bromide for 30 min to stain the DNA. Finally, the stained gel was analysed with a UVITEC Cambridge with a UVIDOC HD2.

The irradiation of the samples was performed in a carousel device inside a photo-activator (Luzchem Research, Inc. Option 1) at 350 nm. In addition, the experiment was repeated twice.

**DNA platination studies.** A2780 ovarian cancer cells were cultured to 70% confluency, the medium was replaced with a medium containing 20  $\mu\text{M}$  of the target metal complex and the cells were further incubated for 4 h. After the treatment the cells were washed with PBS and new fresh complex-free medium was added. Then, one batch of cells was further processed while a second batch was irradiated for 10 min at 350 nm in a Rayonet Irradiation Chamber ( $2.58 \text{ J cm}^{-2}$ ) and then further processed. The cell pellets were collected by trypsinization and further centrifuged at 650g, 4  $^\circ\text{C}$  for 5 minutes (5910R, Eppendorf) and washed two times with ice-cold PBS. DNA was extracted using a DNA extraction kit (illustra BACC1, GE Healthcare) following the manufacturer's procedure. The content of nucleic acid was quantified *via* the 260/280 nm absorbance ratio on a Cary60 UV-Vis spectrophotometer (Agilent Technologies), equipped with an ND-1000 nanodrop system (Witec AG). The DNA aliquots were then lyophilized in an Alpha 2–4 LD plus (CHRIST). The obtained samples were chemically digested for 24 h in a 10% aqua regia solution and further diluted to achieve a 2% solution that was injected in ICP-MS.

ICP-MS measurements were performed on an Agilent QQQ 8800 Triple quad ICP-MS spectrometer (Agilent Technologies) with an ASX200 autosampler (Agilent Technologies), equipped with standard nickel cones and a “micro-mist” quartz nebulizer fed with 0.3  $\text{mL min}^{-1}$  analytic flow (as a 2%  $\text{HNO}_3$  aqueous solution). Platinum was measured against a Pt single element standard (Merck 1703410100) and verified by a

control (Agilent 5188-6524 PA Tuning 2). The platinum content of the samples was determined by means of an 8-step serial dilution in the range between 0 and 200 ppb in Pt ( $R > 0.99$ ) with a background equivalent concentration of BEC: 11.8 ppt and a detection limit of DL: 5.4 ppt. The isotopes  $\text{Pt}^{194}$  (32.97% abundance) and  $\text{Pt}^{195}$  (33.83% abundance) were evaluated in “no-gas” and “He-gas” modes. Spiking the samples with 1% methanol (to account for eventual carbon content from the biological samples) resulted in equivalent values within error ranges. A solution of indium (500 ppb) and tungsten (500 ppb) was used as an internal standard. The results are expressed as ppb Pt per sample.<sup>50,51</sup>

**Pulse field gel electrophoresis studies.** A2780 ovarian cancer cells were cultured to sub-confluency, the medium was replaced with a medium containing the vehicle alone (DMF), cisplatin (cPt, 10  $\mu\text{M}$ ), camptothecin (CMPT 2.5  $\mu\text{M}$ ) or the target metal complex (20  $\mu\text{M}$ ) and the cells were further incubated for 4 h. After the treatment the cells were washed with PBS and new fresh complex-free medium was added. Then, one batch of cells was further processed while a second batch was irradiated for 10 min at 350 nm in a Rayonet Irradiation Chamber (2.58 J  $\text{cm}^{-2}$ ) and then further processed. The cell pellets were collected by trypsinization and further centrifuged at 650g, 4 °C for 5 minutes (5910R, Eppendorf) and washed two times with ice-cold PBS. Agarose plugs of  $10^6$  cells in low melting point agarose (LMP) were prepared in a disposable plug mold (Bio-Rad). The plugs were incubated in lysis buffer (100 mM EDTA, 1% (w/v) sodium lauryl sarcosyl, 0.2% (w/v) sodium deoxycholate, 1 mg  $\text{ml}^{-1}$  proteinase K) at 37 °C for 72 h, and washed three times in 20 mM Tris-HCl pH 8.0, 50 mM EDTA before loading onto an agarose gel. Electrophoresis was performed for 23 h at 14 °C in 0.9% (w/v) Pulse Field Certified Agarose (Bio-Rad CHEF DR III apparatus) containing 0.5% Tris-borate/EDTA buffer. The gel was post-stained with ethidium bromide (EtBr) for 30 min and analyzed using an Alpha Innotech Imaging system and the band intensity was calculated in multiple band mode. The experiments were repeated and one of the two sets was depicted.<sup>52,53</sup>

## Acknowledgements

This work was financially supported by the Portuguese Fundação para a Ciência e Tecnologia (projects PTDC/QUI-QUI/114139/2009, UID/Multi/04349/2013 and EXCL/QEQ-MED/0233/2012 and FCT Investigator grant to FMendes), the Swiss National Science Foundation (Professorships No. PP00P2\_133568 and PP00P2\_157545 to G. G.), the University of Zurich (G. G.), the Stiftung für wissenschaftliche Forschung of the University of Zurich (G. G.), the COST Action CM1105 (G. G., A. Q. and A. P.), the UBS Promedica Stiftung (R. R., G. G.), the Forschungskredit of the University of Zurich (R. R.), the Novartis Jubilee Foundation (R. R., G. G.), the PSL Excellence Chair Program Grant (ANR-10-IDEX-0001-02 PSL to G. G.), the 973 Program (no. 2015CB856301), the National Science Foundation of China (no. 21471164), the China Scholarships

Council (Grant No. 201506380026 to H. H.), and the MINECO (Spain Governmental Agency) GRANT SAF-2012-34424 and CTQ-2015-68779-R. The authors would also like to thank Célia Fernandes for the mass spectrometry analyses, which were carried out on a QITMS instrument, acquired with the support of the Programa Nacional de Reequipamento Científico (Contract REDE/1503/REM/2005-ITN) of FCT and is part of RNEM-Rede Nacional de Espectrometria de Massa. Ana Graça is acknowledged for the gamma camera imaging studies with Pt-LQ-Tc injected BALB/C female mice.

## Notes and references

- 1 T. Gianferrara, C. Spagnul, R. Alberto, G. Gasser, S. Ferrari, V. Pierroz, A. Bergamo and E. Alessio, *ChemMedChem*, 2014, **9**, 1231–1237.
- 2 A. Naik, R. Rubbiani, G. Gasser and B. Spingler, *Angew. Chem., Int. Ed.*, 2014, **53**, 6938–6941.
- 3 A. Leonidova, V. Pierroz, R. Rubbiani, J. Heier, S. Ferrari and G. Gasser, *Dalton Trans.*, 2014, **43**, 4287–4294.
- 4 T. Esteves, F. Marques, A. Paulo, J. Rino, P. Nanda, C. J. Smith and I. Santos, *J. Biol. Inorg. Chem.*, 2011, **16**, 1141–1153.
- 5 G. Mion, T. Gianferrara, A. Bergamo, G. Gasser, V. Pierroz, R. Rubbiani, R. Vilar, A. Leczkowska and E. Alessio, *ChemMedChem*, 2015, **10**, 1901–1914.
- 6 A. Leonidova and G. Gasser, *ACS Chem. Biol.*, 2014, **9**, 2180–2193.
- 7 T. C. Johnstone, K. Suntharalingam and S. J. Lippard, *Chem. Rev.*, 2016, **116**, 3436–3486.
- 8 I. Kitanovic, S. Can, H. Alborzinia, A. Kitanovic, V. Pierroz, A. Leonidova, A. Pinto, B. Spingler, S. Ferrari, R. Molteni, A. Steffen, N. Metzler-Nolte, S. Wolfl and G. Gasser, *Chemistry*, 2014, **20**, 2496–2507.
- 9 A. Kastl, S. Dieckmann, K. Wahler, T. Volker, L. Kastl, A. L. Merkel, A. Vultur, B. Shannan, K. Harms, M. Ocker, W. J. Parak, M. Herlyn and E. Meggers, *ChemMedChem*, 2013, **8**, 924–927.
- 10 S. James, K. P. Maresca, J. W. Babich, J. F. Valliant, L. Doering and J. Zubieta, *Bioconjugate Chem.*, 2006, **17**, 590–596.
- 11 K. A. Stephenson, S. R. Banerjee, T. Besanger, O. O. Sogbein, M. K. Levalada, N. McFarlane, J. A. Lemon, D. R. Boreham, K. P. Maresca, J. D. Brennan, J. W. Babich, J. Zubieta and J. F. Valliant, *J. Am. Chem. Soc.*, 2004, **126**, 8598–8599.
- 12 L. Wei, J. W. Babich, W. Ouellette and J. Zubieta, *Inorg. Chem.*, 2006, **45**, 3057–3066.
- 13 A. Yazdani, N. Janzen, L. Banevicius, S. Czorny and J. F. Valliant, *Inorg. Chem.*, 2015, **54**, 1728–1736.
- 14 T. S. Pitchumony, L. Banevicius, N. Janzen, J. Zubieta and J. F. Valliant, *Inorg. Chem.*, 2013, **52**, 13521–13528.
- 15 M. P. Coogan, R. P. Doyle, J. F. Valliant, J. W. Babich and J. Zubieta, *J. Labelled Compd. Radiopharm.*, 2014, **57**, 255–261.



- 16 K. P. Maresca, S. M. Hillier, F. J. Femia, C. N. Zimmerman, M. K. Levadala, S. R. Banerjee, J. Hicks, C. Sundararajan, J. Valliant, J. Zubieta, W. C. Eckelman, J. L. Joyal and J. W. Babich, *Bioconjugate Chem.*, 2009, **20**, 1625–1633.
- 17 S. R. Banerjee, M. K. Levadala, N. Lazarova, L. Wei, J. F. Valliant, K. A. Stephenson, J. W. Babich, K. P. Maresca and J. Zubieta, *Inorg. Chem.*, 2002, **41**, 6417–6425.
- 18 S. S. Jurisson and J. D. Lydon, *Chem. Rev.*, 1999, **99**, 2205–2218.
- 19 G. R. Morais, A. Paulo and I. Santos, *Organometallics*, 2012, **31**, 5693–5714.
- 20 R. Alberto, K. Ortner, N. Wheatley, R. Schibli and A. P. Schubiger, *J. Am. Chem. Soc.*, 2001, **123**, 3135–3136.
- 21 M. Bartholoma, J. Valliant, K. P. Maresca, J. Babich and J. Zubieta, *Chem. Commun.*, 2009, 493–512.
- 22 C. Moura, T. Esteves, L. Gano, P. D. Raposinho, A. Paulo and I. Santos, *New J. Chem.*, 2010, **34**, 2564–2578.
- 23 D. Can, B. Spingler, P. Schmutz, F. Mendes, P. Raposinho, C. Fernandes, F. Carta, A. Innocenti, I. Santos, C. T. Supuran and R. Alberto, *Angew. Chem., Int. Ed.*, 2012, **51**, 3354–3357.
- 24 G. Lu, S. M. Hillier, K. P. Maresca, C. N. Zimmerman, W. C. Eckelman, J. L. Joyal and J. W. Babich, *J. Med. Chem.*, 2013, **56**, 510–520.
- 25 P. Nunes, G. R. Morais, E. Palma, F. Silva, M. C. Oliveira, V. F. Ferreira, F. Mendes, L. Gano, H. Vicente Miranda, T. F. Outeiro, I. Santos and A. Paulo, *Org. Biomol. Chem.*, 2015, **13**, 5182–5194.
- 26 T. E. Kydonaki, E. Tsoukas, F. Mendes, A. G. Hatzidimitriou, A. Paulo, L. C. Papadopoulou, D. Papagiannopoulou and G. Psomas, *J. Inorg. Biochem.*, 2016, **160**, 94–105.
- 27 R. M. Medina, J. Rodriguez, A. G. Quiroga, F. J. Ramos-Lima, V. Moneo, A. Carnero, C. Navarro-Ranninger and M. J. Macazaga, *Chem. Biodiversity*, 2008, **5**, 2090–2100.
- 28 F. J. Ramos-Lima, O. Vrana, A. G. Quiroga, C. Navarro-Ranninger, A. Halamikova, H. Rybnickova, L. Hejmalova and V. Brabec, *J. Med. Chem.*, 2006, **49**, 2640–2651.
- 29 N. Lazarova, S. James, J. Babich and J. Zubieta, *Inorg. Chem. Commun.*, 2004, **7**, 1023–1026.
- 30 N. Viola-Villegas, A. E. Rabideau, M. Bartholomé, J. Zubieta and R. P. Doyle, *J. Med. Chem.*, 2009, **52**, 5253–5261.
- 31 S. Alves, A. Paulo, J. D. Correia, L. Gano, C. J. Smith, T. J. Hoffman and I. Santos, *Bioconjugate Chem.*, 2005, **16**, 438–449.
- 32 B. M. Still, P. G. Kumar, J. R. Aldrich-Wright and W. S. Price, *Chem. Soc. Rev.*, 2007, **36**, 665–686.
- 33 F. Mendes, L. Gano, C. Fernandes, A. Paulo and I. Santos, *Nucl. Med. Biol.*, 2012, **39**, 207–213.
- 34 J. J. Wilson and S. J. Lippard, *J. Med. Chem.*, 2012, **55**, 5326–5336.
- 35 I. Buss, D. Garmann, M. Galanski, G. Weber, G. V. Kalayda, B. K. Keppler and U. Jaehde, *J. Inorg. Biochem.*, 2011, **105**, 709–717.
- 36 A. Leonidova, V. Pierroz, R. Rubbiani, Y. Lan, A. G. Schmitz, A. Kaech, R. K. O. Sigel, S. Ferrari and G. Gasser, *Chem. Sci.*, 2014, **5**, 4044–4056.
- 37 G. Gasser, A. Pinto, S. Neumann, A. M. Sosniak, M. Seitz, K. Merz, R. Heumann and N. Metzler-Nolte, *Dalton Trans.*, 2012, **41**, 2304–2313.
- 38 G. Gasser, S. Neumann, I. Ott, M. Seitz, R. Heumann and N. Metzler-Nolte, *Eur. J. Inorg. Chem.*, 2011, 5471–5478.
- 39 H. Ishida, S. Tobita, Y. Hasegawa, R. Katoh and K. Nozaki, *Coord. Chem. Rev.*, 2010, **254**, 2449–2458.
- 40 I. Kraljić and S. E. Mohsni, *Photochem. Photobiol.*, 1978, **28**, 577–581.
- 41 R. Schmidt, C. Tanielian, R. Dunsbach and C. Wolff, *J. Photochem. Photobiol., A*, 1994, **79**, 11–17.
- 42 C. Mari, V. Pierroz, R. Rubbiani, M. Patra, J. Hess, B. Spingler, L. Oehninger, J. Schur, I. Ott, L. Salassa, S. Ferrari and G. Gasser, *Chemistry*, 2014, **20**, 14421–14436.
- 43 S. Imstepf, V. Pierroz, P. Raposinho, M. Bauwens, M. Felber, T. Fox, A. B. Shapiro, R. Freudenberger, C. Fernandes, S. Gama, G. Gasser, F. Motthagy, I. R. Santos and R. Alberto, *Bioconjugate Chem.*, 2015, **26**, 2397–2407.
- 44 M. J. Macazaga, J. Rodriguez, A. G. Quiroga, S. Peregina, A. Carnero, C. Navarro-Ranninger and R. M. Medina, *Eur. J. Inorg. Chem.*, 2008, 4762–4769.
- 45 G. L. Cohen, W. R. Bauer, J. K. Barton and S. J. Lippard, *Science*, 1979, **203**, 1014–1016.
- 46 T. C. Johnstone, K. Suntharalingam and S. J. Lippard, *Chem. Rev.*, 2016, **116**, 3436–3486.
- 47 D. D. Perrin and W. L. F. Armarego, *Purification of Laboratory Chemicals*, 3rd edn. 1988, p. 392.
- 48 D. E. Troutner, W. A. Volkert, T. J. Hoffman and R. A. Holmes, *Int. J. Appl. Radiat. Isot.*, 1984, **35**, 467–470.
- 49 C. Mari, V. Pierroz, R. Rubbiani, M. Patra, J. Hess, B. Spingler, L. Oehninger, J. Schur, I. Ott, L. Salassa, S. Ferrari and G. Gasser, *Chemistry*, 2014, **20**, 14421–14436.
- 50 A. Frei, R. Rubbiani, S. Tubafard, O. Blacque, P. Anstaett, A. Felgentrger, T. Maisch, L. Spiccia and G. Gasser, *J. Med. Chem.*, 2014, **57**, 7280–7292.
- 51 N. Chekkat, G. Dahm, E. Chardon, M. Wantz, J. Sitz, M. Decossas, O. Lambert, B. Frisch, R. Rubbiani, G. Gasser, G. Guichard, S. Fournel and S. Bellemin-Laponnaz, *Bioconjugate Chem.*, 2016, **27**, 1942–1948.
- 52 K. Hanada, M. Budzowska, S. L. Davies, E. van Drunen, H. Onizawa, H. B. Beverloo, A. Maas, J. Essers, I. D. Hickson and R. Kanaar, *Nat. Struct. Mol. Biol.*, 2007, **14**, 1096–1104.
- 53 V. Pierroz, R. Rubbiani, C. Gentili, M. Patra, C. Mari, G. Gasser and S. Ferrari, *Chem. Sci.*, 2016, **7**, 6115–6124.